Semiconductors, 2022, Vol. 56, No. 10

Growth of hexagonal boron nitride (hBN) on silicon carbide substrates by the physical vapor transport method

© E.N. Mokhov, V.Yu. Davydov¶, A.N. Smirnov, S.S. Nagaluk

Ioffe Institute,
194021 St. Petersburg, Russia

¶ E-mail: Valery.Davydov@mail.ioffe.ru

Received September 15, 2022
Revised September 23, 2022
Accepted September 26, 2022

The possibility of growing hexagonal boron nitride (hBN) of high structural perfection on hexagonal silicon carbide (SiC) substrates using the physical vapor transport method is demonstrated. The results obtained indicate that this method is promising for the formation of large-area high-quality hBN/SiC heterostructures in the course of one technological process, which have a high potential for device applications.

Keywords: hexagonal boron nitride, high-temperature sublimation from the gas phase, Raman spectroscopy, photoluminescence.

DOI: 10.21883/SC.2022.10.54910.9961

1. Introduction

Hexagonal Boron Nitride (hBN) — a wide-band semiconductor material with a whole set of unique properties has recently aroused great interest in connection with the possibility of creating a new generation of optoelectronic semiconductor devices based on it with improved characteristics [1–3].

The main methods of hBN growth are chemical vapor deposition (CVD) and liquid phase epitaxy (LPE) growth. When growing hBN by the CVD, transition metals — Cu, Ni, Fe, Pt or their alloys are usually used as substrates. It has been established that these metals contribute to the growth of hexagonal hBN. BN synthesis is carried out at atmospheric pressure in an ammonia medium with the addition of borane, borazine or trichloroborane. This method was used to obtain thin, several atomic layers thick, single crystals hBN layers of large area [4], from 10 to 100 cm^2, on metal substrates. The growth temperature in the above methods usually did not exceed 1000°C. For further use, the hBN layers were separated using special mechanical or chemical techniques. The growth of thicker epitaxial layers is hindered by the fact that the metal substrates used have low melting temperatures. Analysis of the conditions for obtaining monocrystals of compounds with a binding energy of (E_b) comparable to E_bhBN shows that growth temperatures of are required for the growth of thick layers or bulk single crystals of hBN$\sim$ 2000°C.

At the moment, there is a high need to obtain hBN layers with thicknesses of > 1 micrometer, since the latter allows obtaining a significant amount of material on an industrial scale with its further use for various instrument applications [5,6]. So, in a number of works, other growth methods were used, for example, the method of liquid-phase epitaxy [7–10]. The growth was carried out in metal melts: Ni [8], Ni−Cr [9] and Fe−Cr [10] with the addition of BN powder. It has been established that in systems containing Ni or Fe, an increase in the thickness of the grown layer is observed. Thus, hBN crystals up to 200 micrometer thick and several millimeters long [9] were obtained from the Fe−Cr melt. It was noted that with an increase in the growth temperature, the structural perfection of crystals improves. The highest-quality monocrystal hBN layers were grown from melts of Ba, Mg and Li containing B and N at elevated pressures and temperatures (NRNT method) [11,12]. For example, in work [12] it was reported about the cultivation of transparent and colorless lamellar single crystals of hBN with a length of 2.5 mm and a thickness of 10 mm at a growth temperature of 2100°C and a pressure of 30 kbar. Unfortunately, this method is technically very complicated and requires special expensive equipment [12]. Epitaxial layers of hBN with a thickness of several microns, with linear dimensions up to 10 mm, were also grown on AlN [13] and AlGaN [5] substrates by the high-temperature chemical deposition (HTCVD) at a growth temperature of 1600°C.

The task of developing growth methods aimed at increasing the thickness and area of high-quality hBN single crystals on wide-band semiconductor substrates is undoubtedly relevant. The purpose of this work — is to develop a technology for growing thick (thickness range 5−20 microns) single crystal hBN layers of a large area by sublimation from the gas phase (PVT) on substrates of a wide-band semiconductor silicon carbide 6*H*-SiC.

2. Experimental part

Growing of hBN crystals was carried out in a resistive heating unit by high-temperature sublimation from the gas phase. The installation is equipped with a cylindrical graphite heater of the meander type, which is installed inside a water-cooled stainless steel chamber, a turbo-

molecular pump controlled by a high-frequency rectifier, a pyrometer of spectral ratio and a system for pumping gas and maintaining pressure during the growth process. The use of a heater and thermal insulation in a growing plant made of graphite can lead to uncontrolled doping of the growing crystal with carbon. Closed containers made of tantalum were used to lower the carbon content in the grown hBN crystals. A silicon carbide wafer, polytype $6H$ ($6H$-SiC), diameter ~ 15 mm, with orientation (0001) Si-face was used as a seed crystal. The source of BN vapors was polycrystalline boron nitride powder of high purity. The distance between the source and the substrate was 1−2 mm. The growing temperature was within 1950−2100°C, nitrogen pressure in the growth chamber varied within 300−700 mm Hg, nitrogen purity was 99.999%. In some experiments, lithium was injected into the growth zone, contributing to an increase in BN mass transfer. The growth rate of the hBN crystal varied from 10 to 50 microns/h.

To reduce the density of crystallization centers in this work, close space growth technique of the method of physical vapor deposition (PVT), known as the Sublimation Sandwich Method (SSM) [14], was used. Currently, SSM is widely used for the growth of high-quality bulk crystals and epitaxial layers of SiC [15], AlN and GaN [16]. Unlike the CVD method, SSM allows growth on various substrates in a wide temperature range 1800−2200°With controlled growth conditions, which is important for optimizing the conditions for obtaining high-quality hBN layers with the required parameters. When using SSM in conditions of low supersaturation, it is easy to implement a step-flow growth mode growth mechanism, which minimizes the occurrence of new incoherent growth centers in the growing process, which is extremely important for obtaining high-quality, low-density dislocations of crystals.

Previous studies [16] have shown that epitaxial layers of AlN grown on a SiC substrate at a temperature ~ 2000°C contain Si and C impurities at the level of 1−10%. A similar level of doping with these impurities can be expected in hBN layers grown on substrates SiC.

The grown epitaxial layers were studied by Raman spectroscopy and photoluminescence. The experiments were carried out on a LabRam HREvo UV-VIS-NIR-Open spectrometer (Horiba, Lille, France) equipped with a confocal microscope and a silicon CCD matrix cooled to liquid nitrogen temperature. The $\lambda = 532$ nm (2.33 eV) Nd:YAG laser line (Torus, Laser Quantum, Inc., Edinburgh, UK) was used to excite the Raman and PL spectra. The laser beam on the sample surface was focused using Olympus lenses $100^\times$ (NA = 0.9) and Leica PL FLUOTAR $50^\times$ (NA = 0.55) into a spot with a diameter of $\sim 1-2$ microns. The spectra were recorded using diffraction gratings of 1800 and 600 grooves/mm. A commercially available monocrystal hBN manufactured by HQ Graphene was used as a reference sample.

Figure 1. The surface of the hBN crystal after growth on the substrate $6H$-SiC.

3. Results and discussion

During the growth process, epitaxial layers of hBN were grown, the diameter of the samples was ~ 15 mm, the thickness varied from 5 to 20 microns. A photo of one of the samples used in our research is shown in Fig. 1.

In order to establish the crystal modification of the grown BN samples, the technique of Raman spectroscopy (Raman scattering) was used. Fig. 2 shows the Raman spectra recorded on a sample grown on a SiC substrate.

The hexagonal BN has spatial symmetry $P6_3/mmc$ (point group D_{6h}). There are two formula units of BN per primitive cell. Boron and nitrogen atoms occupy positions $2c$ and $2d$ respectively. The mechanical representation at the Γ-point of the Brillouin zone can be written as follows: $\Gamma = \Gamma_{ac} + \Gamma_{opt} = 2(A_{2u} + B_{1g} + E_{2g} + E_{1u})$, where $\Gamma_{ac} = A_{2u} + E_{1u}$ and $\Gamma_{opt} = A_{2u} + 2B_{1g} + 2E_{2g} + E_{1u}$. The two vibrational modes are acoustic and 6 modes are optical. Among the optical modes: $A_{2u}$and E_{1u} — infrared-active optical modes, two B_{1g} — IR and Raman-inactive (silent) modes, two E_{2g} — Raman-active optical modes [17]. Thus, the Raman spectrum of hBN must contain two doubly degenerate phonon modes of symmetry E_{2g}. The high-frequency mode $E_{2g}^{(2)}$ is associated with displacements of boron and nitrogen atoms in opposite directions in each plane BN. The low-frequency mode $E_{2g}^{(1)}$ is caused by the movement of two BN planes relative to each other, while in each plane the boron and nitrogen atoms shift in the same direction, which changes to the opposite direction in the adjacent plane. Unambiguous identification of the hexagonal modification BN is usually carried out by detecting both Raman modes: low-frequency $E_{2g}^{(1)}$ at a frequency of 52.5 cm^{-1} and high-frequency $E_{2g}^{(2)}$ at a frequency of 1365.7 cm^{-1} [18]. The Raman spectra shown in Fig. 3, recorded on a sample grown on a SiC substrate, undoubtedly indicate that this sample is a boron nitride of hexagonal modification. Additionally, Fig. 3, *a* also

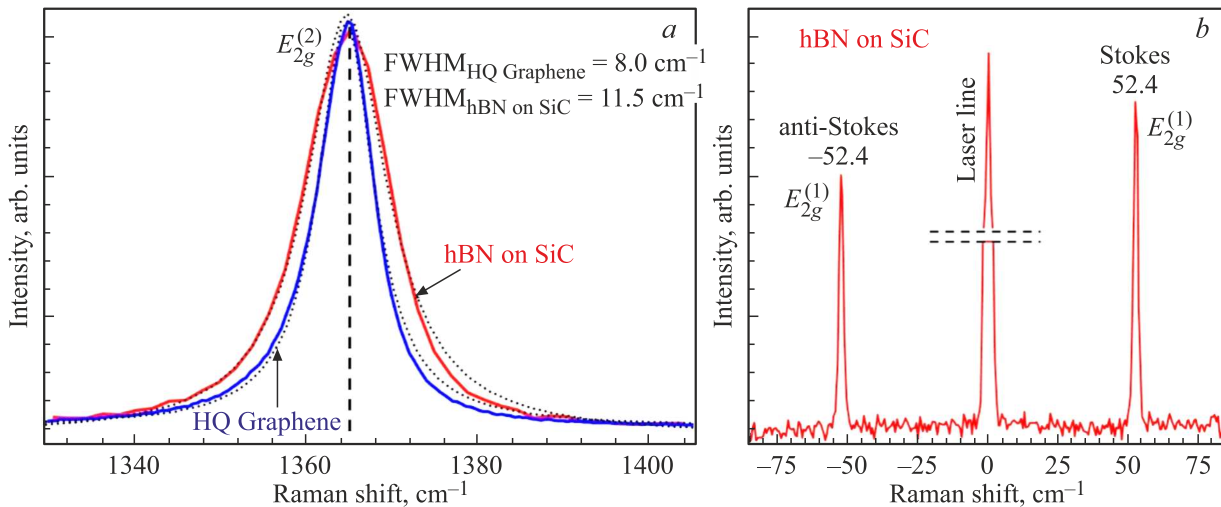

Figure 2. *a* — Raman spectra of hBN in the region of phonon symmetry $E_{2g}^{(2)}$. The blue color shows the spectrum registered on the reference sample hBN (HQ Graphene); the red color indicates the spectrum of the hBN sample grown on SiC. The dots show simulations of Raman peaks by a Lorentz contour with a full-width at half maximum (FWHM) parameter of 8.0 and 11.5 cm^{-1}. The dotted vertical line indicates the position of the maximum of the Raman peaks 1365.2 cm^{-1}, corresponding to the scattering of light on the optical phonon of symmetry $E_{2g}^{(2)}$. *b* — low-frequency Raman spectrum of the hBN sample grown on SiC, registered in both Stokes (52.4 cm^{-1}) and anti-Stokes (−52.4 cm^{-1}) areas of the spectrum.

shows the Raman spectrum registered on the reference hBN comparison sample. It can be seen that the frequency of scattered light is 1365.2 cm^{-1} observed in the spectra of both samples corresponds to the Raman peak of symmetry $E_{2g}^{(2)}$ hBN. The width of this Raman peak at half-height (FWHM), reflecting the lifetime of the optical phonon, is used to assess the structural perfection of a monocrystal hBN. According to the literature data, the FWHM parameter varies in the range from 7.3 cm^{-1} [19] for hBN samples grown by HPHT at the National Institute of Materials Science of Japan (NIMS), up to 14.8−25.0 cm^{-1} for samples grown by the CVD [20]. The parameter FWHM = 11.5 cm^{-1} registered on hBN grown on SiC is close to the parameter FWHM = 8.0 cm^{-1} for a commercially available structurally perfect sample of hBN (HQ Graphene).

After it was shown that the PVT method makes it possible to grow structurally perfect hBN on 6*H*-SiC substrates, its optical properties were investigated by the PL method in order to identify uncontrolled impurities doping the sample during high-temperature growth. Fig. 3 shows the PL spectra recorded at a temperature of 100 K, both on an hBN sample grown on a SiC substrate and on a comparison sample. It can be seen that the comparison sample does not contain obvious signs of impurity photoluminescence, whereas the sample grown on SiC shows a wide band of PL in the visible region of the spectrum (600−780 nm). This band consists of a zero-phonon line (ZPL) with a radiation maximum of $E_{\text{ZPL}} = 1.97$ eV and at least two of its phonon replicas with a characteristic phonon energy of $E_{\text{ph}} = 160$ meV, which corresponds to the maximum density phonon states associated with the plane dispersion of longitudinal (LO) and transverse (TO) optical phonons at *K* and *M* points of the Brillouin zone hBN [21]. A similar PL spectrum was previously observed in bulk hBN as from single defects [22], and from their ensembles [23]. At the same time, in the study [23], a correlation was shown between the appearance of this PL band and the

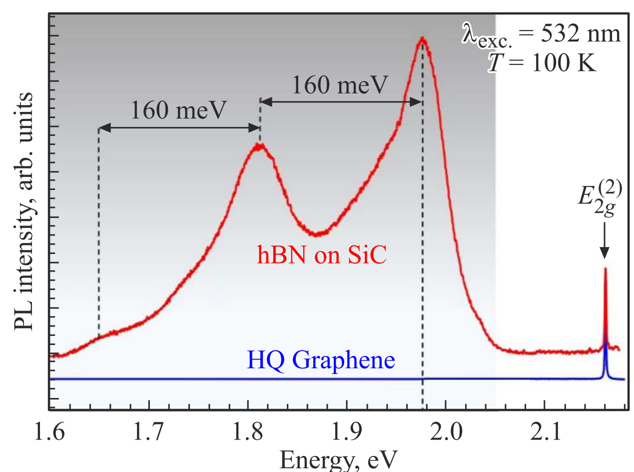

Figure 3. The PL spectrum of the hBN sample grown on a SiC substrate (red spectrum) and the PL spectrum of the hBN HQ Graphene sample (blue spectrum). The vertical arrow indicates the Raman line E_{2g} observed in the spectra of both samples. A wide band corresponding to the PL of defects associated with a carbon impurity is indicated by gray shading. Dotted lines indicate the maximum of the ZPL and its phonon replicas. The spectra were recorded at a temperature of $T = 100$ K, excitation by the Nd:YAG laser line $\lambda = 532$ nm (2.33 eV), and shifted vertically for clarity.

presence of impurity carbon atoms in the hBN lattice. Thus, the presence of this PL band indicates that during high-temperature PVT growth, hBN crystals turn out to be carbon-doped, which can be explained by diffusion from the SiC substrate and from the walls of the growth chamber containing graphite.

It should be noted that the properties of defects associated with carbon impurity in hBN are currently being actively investigated due to several reasons [22–26]. Firstly, it was shown that the PL caused by them is active at room temperature, which makes it possible to create solid-state sources of single photons in this van der Waals material that do not require cryogenic temperatures [22,25]. Secondly, it was found that the PL of defects associated with carbon impurity in hBN is spin-dependent [24], which makes it possible to read the electronic spin state of these defects by optically detectable magnetic resonance (ODMR). The latter opens up the possibility of using carbon impurities in hBN to create quantum sensors of magnetic fields, pressure, temperature and other parameters, as well as quantum bits. Thus, the results obtained by us show the applicability of using the PVT method not only for the growth of hBN, but also demonstrate the possibility of obtaining such crystals with ensembles of defects associated with carbon impurity. The concept of using ensembles of defects with spin-dependent PL at room temperature to create quantum sensors of magnetic fields and temperature has been successfully tested on a negatively charged nitrogen-vacancy defect in diamond and vacancy-type defects in silicon carbide [27–30].

4. Conclusion

The possibility of growth using the method of high-temperature sublimation from the gas phase of hexagonal boron nitride (hBN) of high structural perfection on substrates of hexagonal silicon carbide (SiC) is demonstrated. In this study, the linear size of the grown samples was limited only by the size of the substrate (15 mm), however, the growth method we use allows us to grow monocrystals of SiC up to 4 inches in diameter. The results obtained indicate the prospects of using this method for the formation of high-quality large-area hBN/SiC heterostructures during one technological process, which have a high potential for device applications.

By the PL method, it was found that in the process of high-temperature growth, hBN monocrystals turn out to be doped with a carbon impurity in an uncontrolled manner. Defects associated with the carbon impurity in hBN are currently being actively investigated from the point of view of creating single photon sources based on them. Recently, it has also been shown that the luminescence of such defects in hBN is spin-dependent, which potentially opens up prospects for their use for quantum technologies.

Funding

The work was carried out with the support of state assignments of the Ministry of Science and Higher Education of the Russian Federation to Ioffe Institute (0040-2019-0016) and (0040-2019-0006).

Acknowledgments

The authors express their gratitude to V.A. Soltamov for a fruitful discussion of the results of the study.

Conflict of interest

The authors declare that they have no conflict of interest.

References

[1] H.X. Jiang, J.Y. Lin. ECS J. Solid State Sci. Technol., **6**, Q3012 (2017).
[2] R. Haubner, M. Wilhelm, R. Weissenbacher, B. Lux. In *High Performance Non-Oxide Ceramics II,* ed. by M. Jansen (Springer Berlin Heidelberg, Berlin–Heidelberg, 2002) p. 1.
[3] Y. Li. *Innovative synthesis and characterization of large h-BN single crystals: from bulk to nanosheets Materials* (Université de Lyon, 2019). NNT: 2019LYSEI025.
[4] L. Wang, X. Xu, L. Zhang, R. Oiao, M. Wu, Z. Wang, S. Zhang, J. Liang, Z. Zhang, Z. Zhang, W. Chen, X. Xie, J. Zong, Y. Shan, Y. Guo, M. Willinger, Y. Wu, Q. Li, W. Wang, P. Gao, S. Wu, Y. Zhang, Y. Jiang, D. Yu, E. Wang, X. Bai, Z.-J. Wang, F. Ding, K. Liu. Nature, **570**, 91 (2019).
[5] S. Majety, J. Li, X.K. Cao, R. Dahal, B.N. Pantha, J.Y. Lin, H.X. Jiang. Appl. Phys. Lett., **100**, 061121 (2012).
[6] K.Y. Ma, M. Kim, H.S. Shin. Acc. Mater. Res., **3**, 748 (2022)
[7] J.H. Edgar, T.B. Hoffman, B. Clubine, M. Currie, X.Z. Du, J.Y. Lin, H.X. Jiang. J. Cryst. Growth, **403**, 110 (2014).
[8] K. Yoichi, W. Kenji, T. Takashi. Jpn. J. Appl. Phys., **46** (1R), 311 (2007).
[9] T.B. Hoffman, B. Clubine, Y. Zhang, K. Snow, J.H. Edgar. J. Cryst. Growth, **393**, 114 (2014).
[10] S. Liu, R. He, Z. Ye, X. Du, J. Lin, H. Jiang, B. Liu, J.H. Edgar. Cryst. Growth Des., **17** (9), 4932 (2017).
[11] T. Taniguchi, K.Watanabe. J. Cryst. Growth, **303** (2), 525 (2007).
[12] N.D. Zhigadlo. J. Cryst. Growth, **402**, 308 (2014).
[13] N. Coudurier, R. Boichota, F. Merciera. Phys. Procedia, **46**, 102 (2013).
[14] A.S. Segal, A.N. Vorob'ev, S.Yu. Karpov, E.N. Mokhov, M.G. Ramm, M.S. Ramm, A.D. Roenkov, Yu.A. Vodakov, Yu.N. Makarov. J. Cryst Growth, **208**, 431 (2000).
[15] A.A. Lebedev, P.A. Ivanov, M.E. Levinshtein, E.N. Mokhov, S.S. Nagalyuk, A.N. Anisimov, P.G. Baranov. Phys. Usp., **62**, 754 (2019).
[16] E.N. Mokhov, A.A. Wolfson. In *Single Crystals of Electronic Materials: Growth and Properties,* ed. by R. Fornari (Woodhead Publishing, 2018) p. 401.
[17] R. Geick, C.H. Perry, G. Rupprecht. Phys. Rev., **146**, 543 (1966).
[18] T. Kuzuba, K. Era, T. Ishii, T. Sato. Solid State Commun., **25**, 863 (1978).

[19] L. Schué, I. Stenger, F. Fossard, A. Loiseau, J. Barjon. 2D Mater., **4**, 015028 (2017).
[20] K. Ahmed, R. Dahal, A. Weltz, J.-Q. Lu, Y. Danon, I.B. Bhat. Appl. Phys. Lett., **109**, 113501 (2016).
[21] G. Kern, G. Kresse, J. Hafner. Phys. Rev. B, **59**, 8551 (1999).
[22] L.J. Martinez, T. Pelini, V. Waselowski, J.R. Maze, B. Gil, G. Cassabois, V. Jacques. Phys. Rev. B, **94**, 121405(R) (2016).
[23] M. Koperskia, D. Vaclavkova, K. Watanabe, T. Taniguchid, K.S. Novoselova, M. Potemski. PNAS, 117, 13214 (2020).
[24] H.L. Stern, Q. Gu, J. Jarman. S.E. Barker, N. Mendelson, D. Chugh, S. Schott, H.H. Tan, H. Sirringhaus, I. Aharonovich, M. Atatüre. Nature Commun., **13**, 618 (2022).
[25] N. Mendelson, Z.-Q. Xu, T.T. Tran, M. Kianinia, J. Scott, C. Bradac, I. Aharonovich, M. Toth. ACS Nano, **13** (3), 3132 (2019).
[26] P. Auburger, A. Gali. Phys. Rev. B, **104**, 075410 (2021).
[27] L. Childress, R. Walsworth, M. Lukin. Phys. Today, **67** (10), 38 (2014).
[28] H. Zheng, J. Xu, G. Z. Iwata, T. Lenz, J. Michl, B. Yavkin, K. Nakamura, H. Sumiya, T. Ohshima, J. Isoya, J. Wrachtrup, A. Wickenbrock, D. Budker. Phys. Rev. Appl., **11**, 064068 (2019).
[29] S.A. Tarasenko, A.V. Poshakinskiy, D. Simin, V.A. Soltamov, E.N. Mokhov, P.G. Baranov, V. Dyakonov, G.V. Astakhov. Phys. Status Solidi B, **255**, 1700258 (2018).
[30] S. Castelletto, A. Peruzzo, C. Bonato, B. C. Johnson, M. Radulaski, H. Ou, F. Kaiser, J. Wrachtrup. ACS Photonics, **9** (5), 1434 (2022).